



Deep Learning-Based Faults Detection and Classification in Photovoltaic Systems Using Voltage and Current Images

Izziyyah M. Alsudi¹, Mohammad Abulaila² , Kasim M. Al-Aubidy^{3*} 

^{1,2} Mechatronics Engineering Department, Al-Balqa Applied University, Jordan

³ Mechatronics Engineering Department, Tishk International University, Erbil, Iraq

E-mail: qasim.obaidi@tiu.edu.iq

Received: Nov 16, 2023

Revised: Feb 19, 2024

Accepted: Feb 27, 2024

Available online: Aug 19, 2024

Abstract— There is a significant growth in the use of solar photovoltaics (PV) for clean and sustainable renewable energy. The ease of installation and expansion of PV power plants makes them suitable for grid-connected operation. However, increasing the size of the PV power plant will make it difficult to detect and classify faults, which leads to lower system efficiency and reliability. Therefore, this article proposes a method for detecting and classifying faults in PV systems in order to fix them more quickly and efficiently. For this purpose, the data of current and voltage are collected from every panel for a period of time in normal case and for three common fault types (open circuit, short circuit, and shading), and afterwards converted into wavelet transform images. Then a deep learning approach is used to detect, classify, and locate defective panels in a PV system. The obtained results show that the deep learning approach based on Resnet50, and voltage images was 100% accurate compared to the deep learning approach based on current images. In this methodology there is no need for additional sensors since they are embedded with panels and sent to main computer. Since the voltage parameter has the best accuracy scenario, it is converted to images, then ResNet-50 is applied. So, every panel can be detected and classified, and as each panel is numbered, the fault location can be readily determined.

Keywords— Convolutional neural network; Deep learning; Photovoltaic systems; Faults detection and classification; Real-time monitoring.

1. INTRODUCTION

Recently, renewable energy sources are increasingly being used to generate clean, sustainable energy instead of traditional fuels. Solar energy is the main source of renewable energy for generating electricity. PV cells are spread over large areas and in remote areas. Therefore, there must be a way to detect and diagnose faults in PV systems in order to repair them more quickly and efficiently. Therefore, specialists in the field of renewable energy have tried to apply artificial intelligence (AI) concepts to design methods for detecting faults in grid-connected PV systems [1].

In PV systems, faults may occur for both alternating current (AC) and direct current (DC) sides [2]. AC side faults relate to problems that typically occur after the DC power generated by the PV panels is converted to AC power by the inverter. While DC side faults occur in the PV system before the DC power is converted into AC power by the inverter. In fact, the inverter fault reduces the AC output power, but does not affect the DC output power [3]. Such faults can disrupt the operation of the PV system, reduce its efficiency, and in cases may pose safety risks. Faults in PV arrays can be caused by physical, electrical, or environmental factors. For example, external damage is caused by cracks in PV modules or degradation [4]. Despite the

use of protection devices, such as circuit breakers, surge protection devices, and ground fault detection, PV systems still need to use advanced methods to detect and diagnose faults using statistical and computational methods or artificial intelligence-based algorithms [2].

Faults on the DC side of PV arrays can occur because of electrical, physical, or environmental factors. The fault may be due to cracks in the PV modules or damage to the PV module or bypass diode [4]. There are four common types of electrical faults: open circuits, line-to-line faults, arc faults, and ground faults. An open circuit fault may occur due to a cracked PV cell or module, or it may occur between the module's interconnections. While line-to-line faults occur when two points have different voltage potentials and accidentally short circuit [5, 6].

An arc fault is a high-energy discharge of electricity that occurs across an air gap between conductors [7]. An arc fault occurs when there is an interruption in the current path due to a broken or a loose connector, or due to mechanical damage or failure of the PV module [8]. As for a ground fault, it occurs when a current-carrying conductor accidentally connects to an equipment-grounding [7, 9]. Environmental faults occur because of temporary or permanent shading. Temporary shading occurs when PV arrays are partially shaded and/or have non-uniform temperatures. Permanent shading occurs when a defective bypass diode or PV module causes a hot spot [4]. In series connected PV modules, a hot spot point occurs when their electrical properties differ, causing the string to overheat [6].

In large-scale PV systems, solar panels are spread over large areas and in remote areas, so Internet of Things (IoT) technology is essential to collect data for monitoring and control purposes [10, 11]. The IoT provides huge data from PV systems that are difficult to handle in traditional ways, especially in real-time applications. Modern computer and communication technologies have encouraged researchers to design algorithms to diagnose faults in PV systems. Some have used soft computing tools, such as fuzzy logic [12] and neural networks [13, 14], to design algorithms for fault detection in PV systems. Others use AI concepts to design machine learning models to predict the behavior of PV systems with the aim of detecting faults based on real-time data provided by IoT devices [15-18].

This research will focus on using deep learning techniques to classify and identify faults in PV systems. Two deep learning models will be presented, the first based on current parameters and the second based on voltage parameters. The rest of the paper is organized as follows: Section 2 presents fault detection methods. This is followed by modeling and simulation of a specific PV system in Section 3. The fourth section discusses the methodology used to detect and locate faults. The fifth section presents the design and testing of the proposed deep learning models, in addition to the results that enhance efficiency and accuracy in detecting faults. Finally, Section 6 deals with the conclusions.

2. FAULTS DETECTION METHODS

Several methods have been proposed for fault detection in PV systems, some of which used traditional fault detection methods, while others relied on artificial intelligence concepts to create intelligent algorithms [19, 20].

2.1. Traditional Methods

Traditional methods of fault detection in PV systems are mainly based on simple measurements and calculations. Thermal imaging has been used to identify hot spots caused

by faults in PV systems. Infrared light is an effective method for detecting and classifying faults in PV systems [21]. Infrared cameras are used to characterize various electrical components and PV modules without the need for sensors. Joule heating is produced by shunted cells, weak connections and short circuits [22, 23]. Electroluminescence imaging technology has also been used to detect faults in PV cells by providing their characteristics in a short period of time [24]. There is a proportional relationship between the emission intensity and the carrier lifetime density in electroluminescence images [20]. In addition, this method can be used to detect other faults, such as unbalanced current distributions, cracks in cells, and faulty connections. In remote and restricted areas, faults in PV modules can be detected using drones [25].

The current-voltage (IV) characteristics of PV modules are used in fault detection by monitoring the behavior of the PV system. In normal operation, IV characteristics follow a certain curve, which changes when a fault occurs. It is clear that the IV characteristics are greatly affected by the type of faults in PV systems. One common method for detecting and classifying photoelectric faults is to compare the fourth characteristic of healthy and defective systems [26]. In addition, Madeti and Singh [20] proposed a voltage/current spectrum analysis method to detect arc faults through low-frequency content analysis. In other attempts, a power loss analysis method was proposed to detect faults in PV systems, where both the model-based PV system and the actual setup of the PV system are used to calculate the power losses. Solórzano and Egido [27] detected and classified DC power losses based on shading, hot spots, degraded units, and cabling problems.

Other traditional methods of fault detection are using sensors to collect and analyze data in real time. Although these methods are relatively simple and can detect common faults, they may not detect sudden problems. Therefore, researchers and specialists moved to use the concepts of artificial intelligence to create intelligent algorithms to detect and diagnose faults in PV systems.

2.2. Smart Methods

Traditional methods are still used to detect and maintain faults in PV arrays, and these methods are ineffective in large-scale systems as they require human effort and take a long time [28]. Therefore, many research and studies have addressed the use of IoT technology, in addition to proposing algorithms for detecting faults [12].

Currently, smart methods are proposed to provide more accurate and efficient faults detection. These methods are based on the concepts of artificial intelligence, machine learning, cloud computing, and IoT technology. These methods are more suitable for large-scale PV systems as they provide accuracy, reliability and efficiency in fault detection and classification [2].

A rule-based fuzzy algorithm was developed by Ducange et. al. [29] to detect faults in PV systems by monitoring the instantaneous power production of the PV system in normal operation. The fuzzy algorithm was trained using data collected during normal operation of the PV plant simulation. A limitation of this method was the false detection of line-to-line and line-to-ground errors under partial shading.

A neural network-based fault diagnosis method for PV systems was presented by Chine et. al. [30]. Two algorithms were used to detect and classify eight different faults. Three inputs are required: the solar irradiance, the PV module temperature, and the PV array current and voltage. Results show that this technique is highly capable of identifying and localizing

different kinds of faults. Aziz et al. [31] presented an intelligent approach that uses convolutional neural networks to extract features from measurement generated by PV system data to detect and classify PV system faults. Artificial intelligence algorithms are used to process big data generated by IoT devices to model fault detection in PV systems. Furthermore, Bonsignore et. al. [32] proposed fuzzy logic and neural networks to model the behavior of a PV system. This method relies on real-time data and the ability of fuzzy systems to establish relationships between input and output variables. Therefore, the Adaptive Neural Fuzzy Inference System (ANFIS) was chosen. The temperature of the module, global irradiances, open circuit voltages, short-circuit currents, as well as the voltage and current at maximum power were monitored. Possible faults can be identified based on the predicted versus obtained curves. This method cannot detect faults online, therefore periodic system checks are required instead.

Recently, deep learning has recently received significant research efforts in various fields and applications, including fault detection [33]. A deep learning model is a hierarchical learning structure, in which complex nonlinear functions are used [34].

To detect errors in the PV system based on deep learning, aerial images obtained from drones were used. In this case, convolutional neural networks (CNNs) are trained to extract high-level features from images and classify faults [35]. A deep learning model was also used to detect and classify six faults on the direct current (DC) side of the PV system. Three electrical indices were used as input to the CNN-based classification model [36]. Du et al. [37] used thermal imaging and CNN to classify defects in silicon PV cells to identify broken edges, surface impurities, scratches, cracks, hot spot and large-scale damage. While Li et al. [33] proposed a deep learning approach to recognize defect patterns using drone aerial images. To classify module defects, convolutional neural networks in machine learning were used. The obtained results confirmed its effectiveness in detecting dust shading faults, erosion of grid lines, and spiral paths on PV modules. In another attempt, Li et.al. [38] used deep CNNs for fault detection in PV systems. It has been used to detect yellowing, delamination, snail trails and dust shading faults. The limitation of this approach is that it cannot detect short circuits and open circuits. Chen et al. [39] proposed a deep residual network for fault detection and diagnosis of PV arrays using current-voltage curves and ambient state data. This method can detect PV array faults, such as partial shading, degradation, short circuits and open circuits. The main contribution of this study focuses on the use of IoT technology to collect data from sensors located in PV panels. Table 1 summarizes a selected sample of faults detection studies and their limitations. The proposed system does not require additional sensors. The limitation of using drones because of regulations and restrictions.

Most previous studies focused on detecting and diagnosing faults, and in this study the location of the faulty panel in the PV system will be determined. The location of the fault is important when the PV system is large-scale or in rural areas. This method determines the specific location of the faulty panel. IoT sensors send data to the main computer used to monitor the PV system, detect, classify and locate faults.

3. PV SYSTEM MODELING AND SIMULATION

To apply this method, a PV system with 4 strings; each consisting of 5 panels in series to achieve a power of 4.2 kW was chosen. Table 2 shows the characteristics of the PV panel, while Table 3 shows the output current, voltage and power of the PV system.

Table 1. Summary of faults diagnosis studies.

| Ref. | Type of fault | Diagnosis | Method | Limitation |
|------|---|--------------------------|---|---------------------------|
| [21] | Hotspot, soldering problem, shading, cabling problems, heated junction box, module breakage, breaker faults | Detect, classify, locate | Thermal imaging through using of lift, walking, and drone | Limitation in using drone |
| [25] | Cracks/broken cells, interconnections problem, shunted diode | Detect, classify, locate | Electro-luminescence, image processing | Limitation in using drone |
| [37] | Defective module | Detect, classify, locate | CNN | Limitation in using drone |
| [26] | Open module in strings | Detect, classify, locate | Time domain reflectometry (TDR), earth capacitance measurement | One type of faults |
| [27] | Partial shading, dirt, hot-spot, module degradation, and power losses due to cabling problems | Detect, classify | Normalized MPP calculation for detection, rule-based approach | Cannot locate |
| [2] | Shading Fault | Detect, locate | CNN | Cannot classify |
| [12] | Shading Fault, Disconnected module | Detect, locate | Fuzzy Logic | Cannot classify |
| [29] | Broken cell, gradual shading, water infiltrations | Detect | Fuzzy Logic | Cannot classify or locate |
| [30] | Faults in module, connection resistance fault, partial shading | Detect, classify | ANN | Cannot locate |
| [32] | Ground fault, diod short circuit, partial shading | Detect | ANFIS | Cannot classify or locate |
| [31] | Line to line fault, Open circuit fault, Partial Shading, fault in Partial Shading and arc fault | Detect, classify | CNN | Cannot locate |
| [33] | dust shading, encapsulated delamination, gridline corrosion, snail trails, and yellowing | Detect, classify | CNN | Cannot locate |
| [35] | Burn marks, delamination, discoloration, glass breakage, and snail trail | Detect, classify | CNN | Cannot locate |
| [36] | Partial shading, L-L, open circuit | Detect, classify | CNN | Cannot locate |
| [38] | Yellowing, delamination, snail trails, dust-shading faults. | Detect | Deep Convolutional Neural Network with Multiple Classification Support Vector Machine | Cannot locate |

Table 2. PV panel parameters.

| Parameter | Value |
|--|--------|
| Maximum Power [W] | 213.15 |
| Cells per Module (N_{cell}) | 60 |
| Open Circuit Voltage V_{oc} [V] | 36.2 |
| Short-Circuit Current I_{sc} [A] | 7.84 |
| Voltage at Maximum Power Point V_{mpp} [V] | 29 |
| Current at Maximum Power Point I_{mpp} [A] | 7.35 |

Table 3. PV system parameters.

| Parameter | Value |
|---------------------|-------|
| Maximum Power [W] | 4200 |
| Voltage [V] | 181 |
| Current [A] | 31.36 |
| Panels in series | 5 |
| Strings in parallel | 4 |

Fig. 1 shows the implemented model of the PV system using MATLAB/Simulink. Each panel has radiation and temperature as inputs and has voltage, current, radiation and temperature as measured outputs. Current and voltage data were collected and analyzed in normal conditions and when faults occurred.

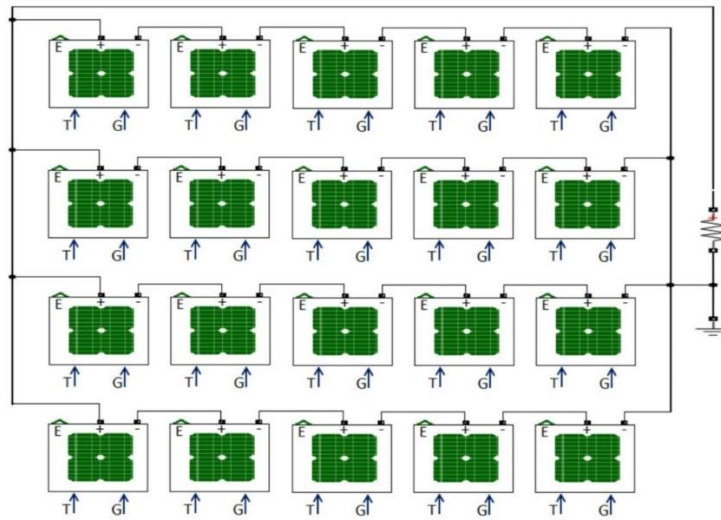


Fig. 1. General layout of the PV system.

4. METHODOLOGY

The methodology used in this study is shown in the flowchart shown in Fig. 2.

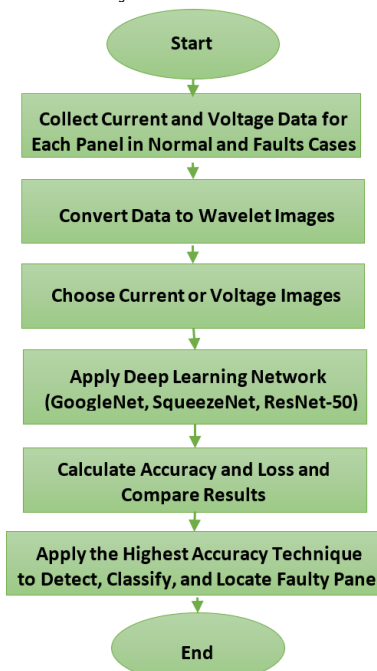


Fig. 2. Faults detection methodology.

The PV system outputs for each panel are voltage and current. In this study, the required data were collected from a PV system simulation for 10 s. Initially, data were collected in the normal condition (no faults), as well as when faults occurred in each panel as in Sections 4.1 and 4.2, respectively. The data will be analyzed, filtered, and converted to wavelet images as described in Section 4.3.

Three types of deep learning networks (GoogleNet, SqueezeNet, and ResNet-50) were applied to the current and voltage images. The results obtained when using current or voltage images were compared to determine the appropriate technique with the highest accuracy.

4.1. Faults Simulation

There are four conditions diagnosed in each panel, as shown in Table 4. Normal condition is tested when there are no faults in all PV panels. An open circuit fault is tested when only one PV panel is disconnected. Short circuit fault is tested when only one PV panel is shorted, and shading fault is tested when only one PV panel is shaded by 200 W/m^2 . The PV system is simulated in an ideal condition without taking into account measurement errors, disturbance or noise.

Table 4. Number of tested cases for each fault.

| Fault | Number of tested cases for the whole system |
|----------------------|---|
| Normal case (Normal) | 1 |
| Open circuit (OC) | 20 |
| Short circuit (SC) | 20 |
| Shading (SH) | 20 |

4.2. Data Collection

In order to train and test fault detection methods, large amounts of photoelectric data are needed. In most cases, this data is collected under specific circumstances. In this work, the data from each panel represents temperature (T), irradiation (G), voltage (V) and current (I). Data from strings representing current and voltage, while data from load, representing current, voltage and power (P), are collected in real time as a 10 s time series, with a sampling time of 0.1 s for simulation purposes. These data are collected by wireless sensors with IoT technology embedded with each PV panel.

Data is collected under many different conditions with different failure states:

- Normal condition: Data is collected without any faults under standard test conditions with irradiance of 1000 W/m^2 and temperature of 25°C , as given in Fig. 3(a).
- Open Circuit Fault: An open circuit is made for one panel in the string and is tested for every panel in the system. Each panel shorted alone and data are collected for each condition under standard test conditions. For the given PV system the number of situations are twenty. When one panel is separated, all panels in the same series are separated. In this case, every panel in the string has an open circuit fault, as shown in Fig. 3(b).

- Short circuit fault: One panel in the string is short-circuited and tested for each panel in the system, as shown in Fig. 3(c). Each panel is shaded individually and data are collected for each case under standard test conditions. The number of situations are twenty.
- Shading Fault: Shading is done at a rate of 200 W/m² for one panel in the string and tested for each panel in the system, as given in Fig. 3(d). Other panels are tested with standard testing conditions. Shaded fault data is collected in twenty situations. Table 5 below shows the data for panels included number of panels when each fault is tested.

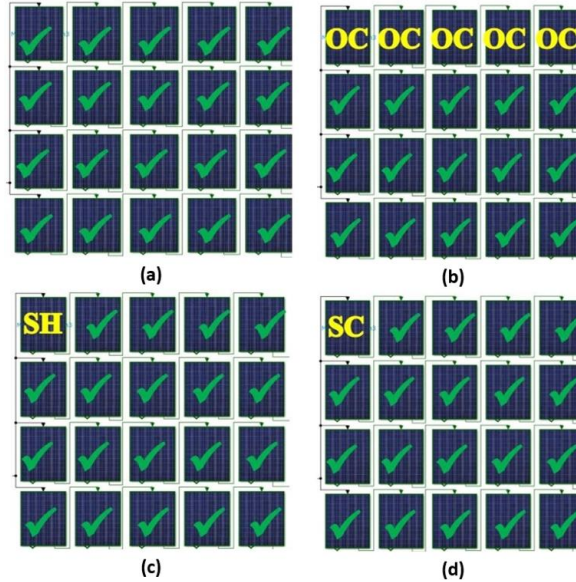


Fig. 3. Status of all panels in the PV system: a) normal case; b) open circuit fault; c) shading fault; d) short circuit fault.

Table 5. Number of faulty and normal panels in all cases.

| Fault | No. of status tested in each case | No. of panels in status for each tested case | No. of normal panels | No. of open circuit panels | No. of short circuit panels | No. of shaded panels |
|---------------------|-----------------------------------|--|----------------------|----------------------------|-----------------------------|----------------------|
| Normal case | 1 | 20 | 20 | - | - | - |
| Open circuit fault | 20 | 5 | 300 | 100 | - | - |
| Short circuit fault | 20 | 1 | 380 | - | 20 | - |
| Shading fault | 20 | 1 | 380 | - | - | 20 |
| Sum | | | 1080 | 100 | 20 | 20 |

When the condition is normal, all panels in all strings are in normal condition. Tested once when all panels are at 1000W/m² and at 25°C. There are 20 panels in normal mode. While applying open circuit fault, all panels in the string that have a panel fault are also in open circuit fault. There are 5 faulty panels in each fault condition and 15 panels in the normal condition. When it is tested for all panels in the system, the total number of panels in open circuit is 100 panels (5*20), and 300 panels (15*20) in normal condition.

In the event of a short circuit, when one of the panels is shorted, the other panels are in a normal state. There is only one panel has short circuit fault and the other 19 panels are in normal condition. When it is tested for all panels in the system (1*20), the sum of panels in short circuit fault is 20 panels and 380 panels (19*20) in normal condition. Same strategy for shading fault, when one panel is shaded, the other panels are in normal condition. Only one panel has shading fault and the other 19 panels are in normal condition. When it is tested for all panels in the

system, the total panels in shading fault are 20 panels and 380 panels in normal condition. The number of normal and faulty panels counts by converting them into images for use in deep learning. The collected data shows the voltage and current in the time series over 10 s with a sampling time of 0.1 s for simulation purposes.

Fig. 4 shows the comparison of the current in the first panel of the first string between 4 different cases. It shows that the current in the normal state fluctuates around a value of 6.60 A and is zero when there is an open circuit. Furthermore, the current is 7.84 A when there is a short circuit, and the average current when there is shading is about 0.50 A. While, Fig. 5 shows the voltage comparison of the first panel of the first string between 4 different cases. The voltage in normal condition fluctuates around 31.70 V and it is 36.20 V in open circuit condition. It is also zero when there is a short circuit and around -0.5 V when there is shading.

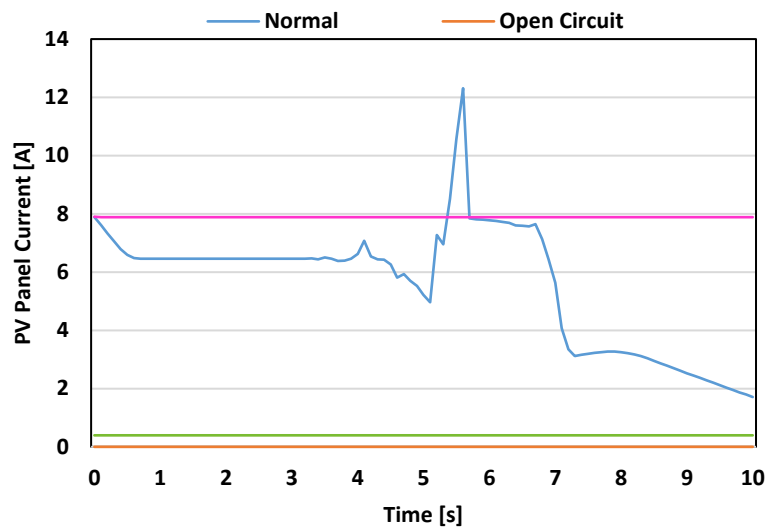


Fig. 4. Current in first panel of first string in normal, open circuit, short circuit, and shading cases.

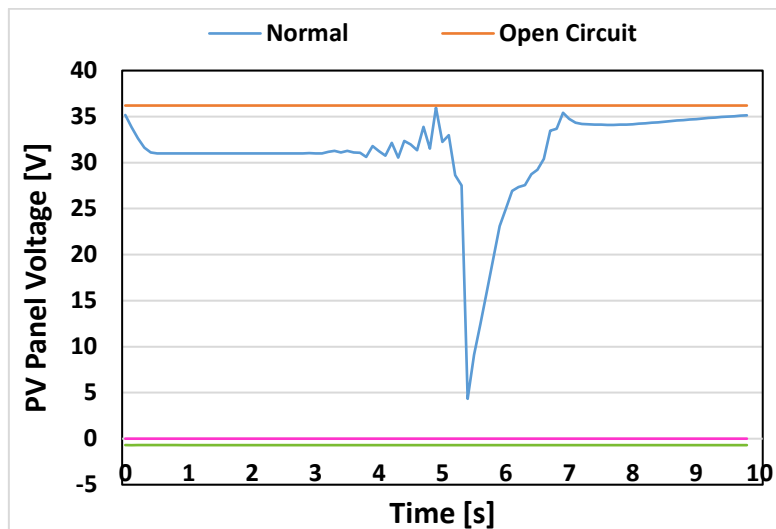


Fig. 5. Voltage in first panel of first string in normal, open circuit, short circuit, and shading cases.

4.3. Feature Extraction Technique

In order to use the deep learning with image classification, a continuous wavelet transform (CWT) is used to convert the data into an image. Wavelet transformation is an effective feature extraction technique used to exploit image features from coarse to fine scales [40]. Continuous wavelet transform has been used in this paper to create a scalogram image of

the time series data collected from each panel, and then apply deep learning to find the extraction features for each fault and normal condition.

The collected current and voltage data is filtered using MATLAB's filter bank and converted to continuous wavelet transform. When a filter bank is used, high accuracy is achieved. An example of the current wavelet transform is shown in Fig. 6, and the voltage wavelet transform is shown in Fig. 7.

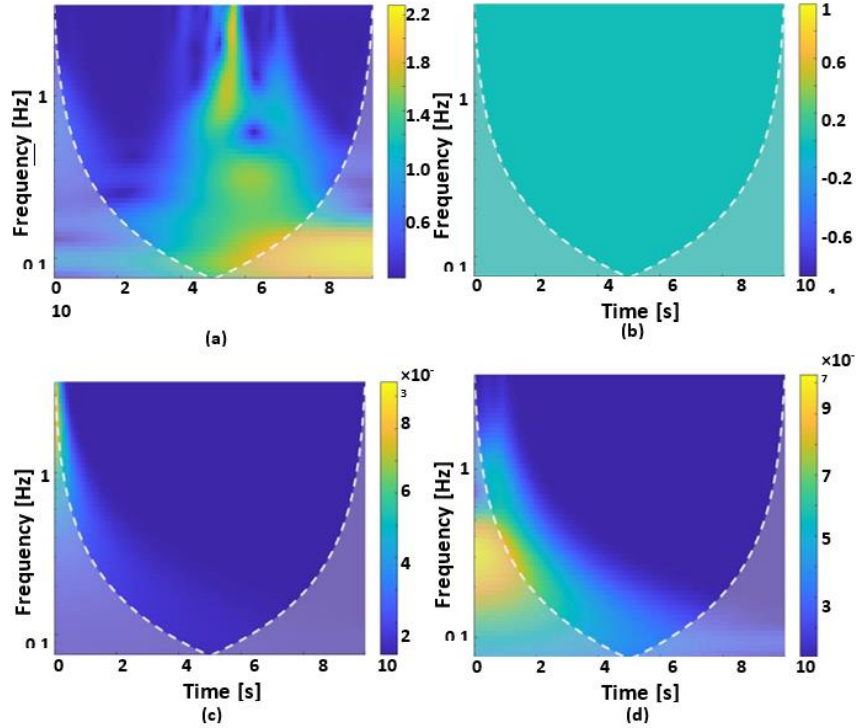


Fig. 6. Example of the wavelet transform of current for a panel in each case: a) normal case; b) open circuit fault; c) shading fault; d) short circuit fault.

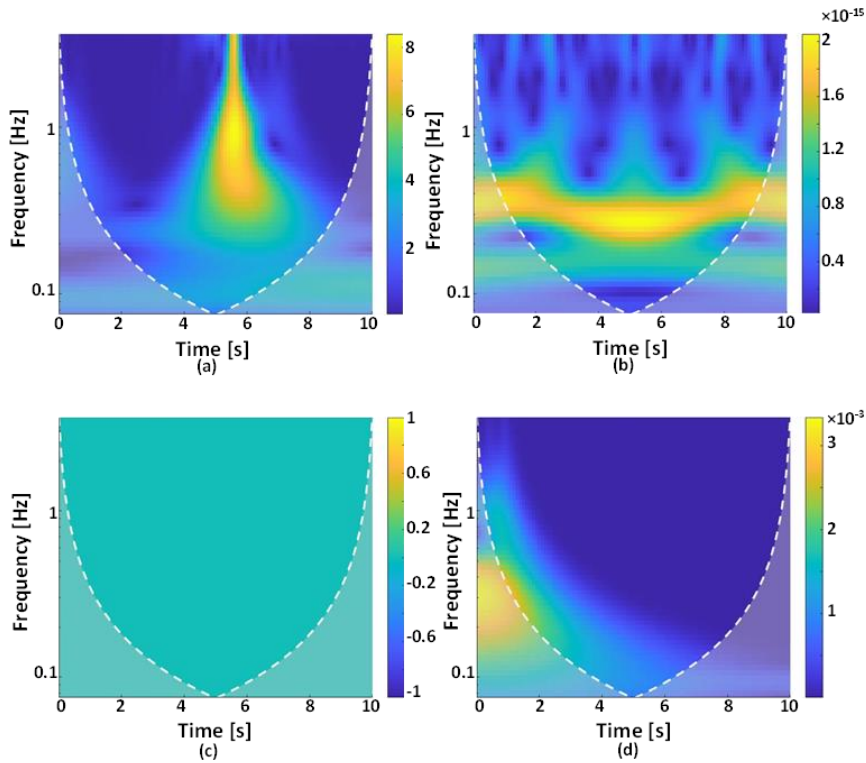


Fig. 7. Example of the wavelet transform of voltage for a panel in each case: a) normal case; b) open circuit fault; c) shading fault; d) short circuit fault.

The continuous wavelet transform converted to jet color map. The jet color map is returned as a three-column array containing the same number of rows as the color map of the current figure. Each row in the array contains the red, green, and blue for a particular color. When trying this technique without using a jet color map, the accuracy and verification does not reach 80%. Figs. 8 and 9 show an example of the current and voltage wavelets in the jet color map respectively for the first panel when it is in the normal, short circuit, open circuit, and shading cases.

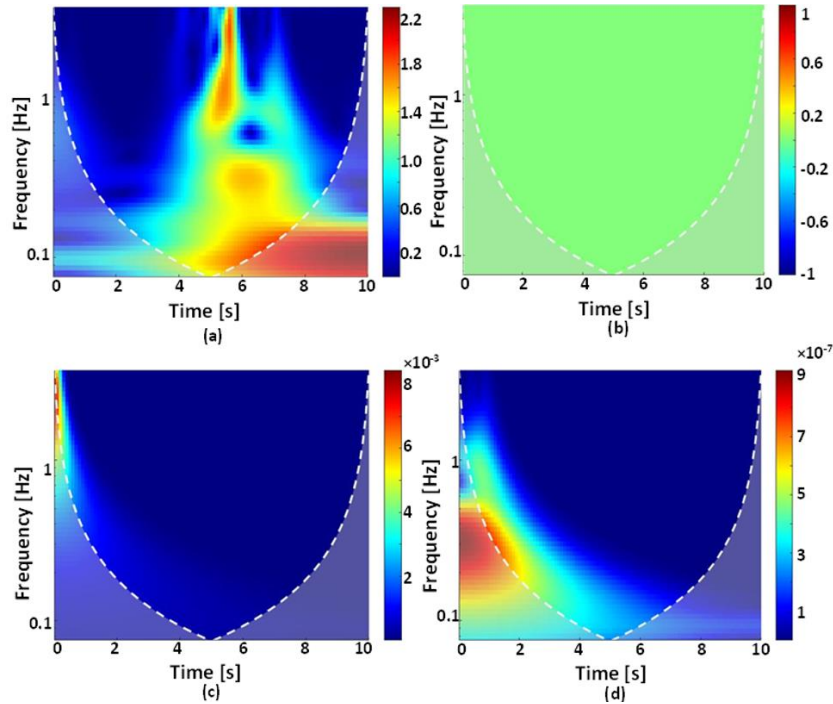


Fig. 8. Example of the wavelet transform of current in jet color map for a panel in each case: a) normal case; b) open circuit fault; c) shading fault; d) short circuit fault.

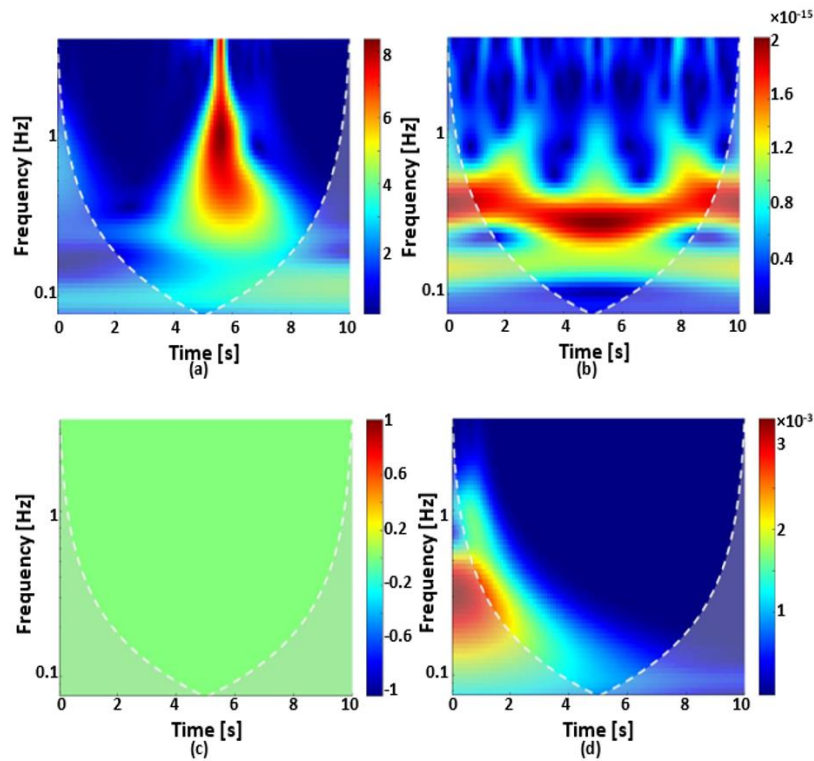


Fig. 9. Example of the wavelet transform of voltage for a panel in each case: a) normal case; b) open circuit fault; c) shading fault; d) Short circuit fault.

When a fault is applied to a PV panel in a string, this fault affects the other panels in the string and the entire system. Fig. 10 shows the voltage wavelet in the jet color map of the whole system in the normal case, all of panels in this figure are normal. Deep learning can extract features for the wavelet image of normal case. Fig. 11 shows an example of a voltage wavelet when an open-circuit fault is applied to the first panel of the first string, and all panels in the same string are in open-circuit mode and have the same wavelet image.

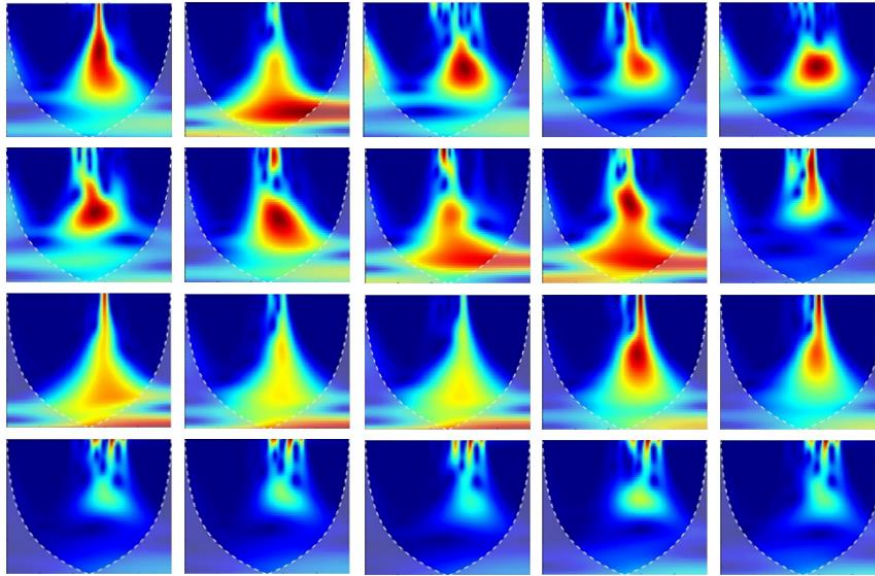


Fig. 10. Voltage wavelet images of PV system panels in normal case.

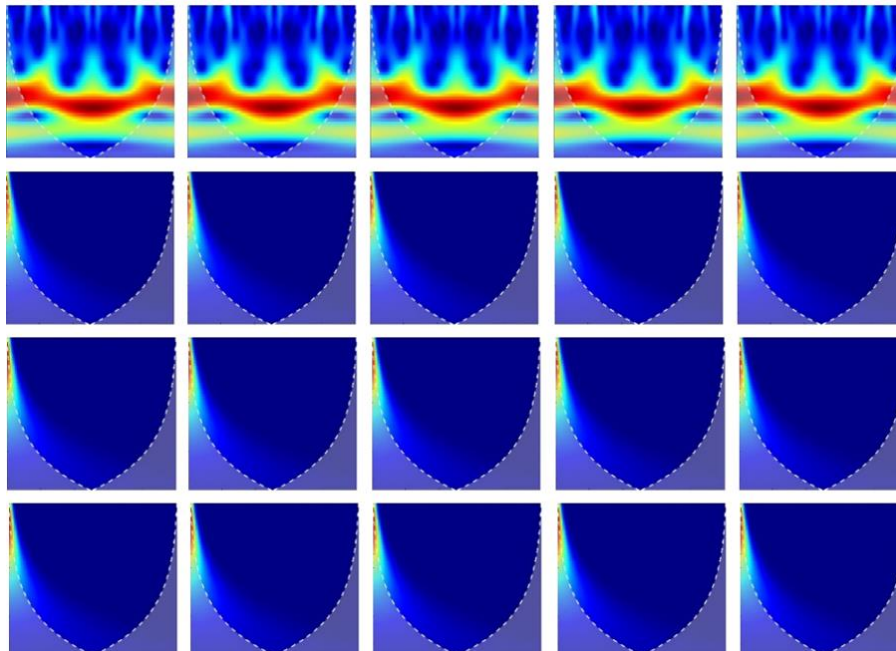


Fig. 11. Voltage wavelet images of the PV system panels for open-circuit fault.

Fig. 12 shows the voltage wavelet when the short-circuit fault is applied to the first panel of the first string, which shows that the image of the panel with the short-circuit fault is different from other panels, and has its own features. While, Fig. 13 shows the voltage wavelet when the shading fault is applied to the first panel of the first string, and it shows that the image of the panel with the shading fault is different from the other panels.

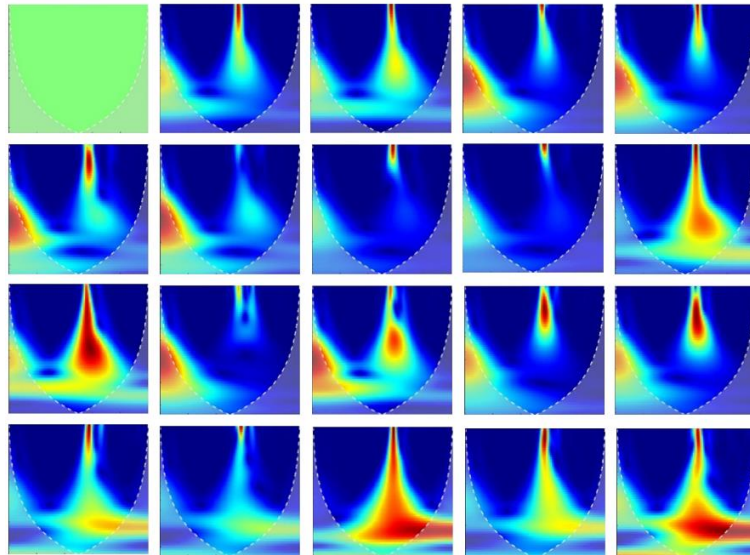


Fig. 12. Voltage wavelet images of the PV system panels for short circuit fault.

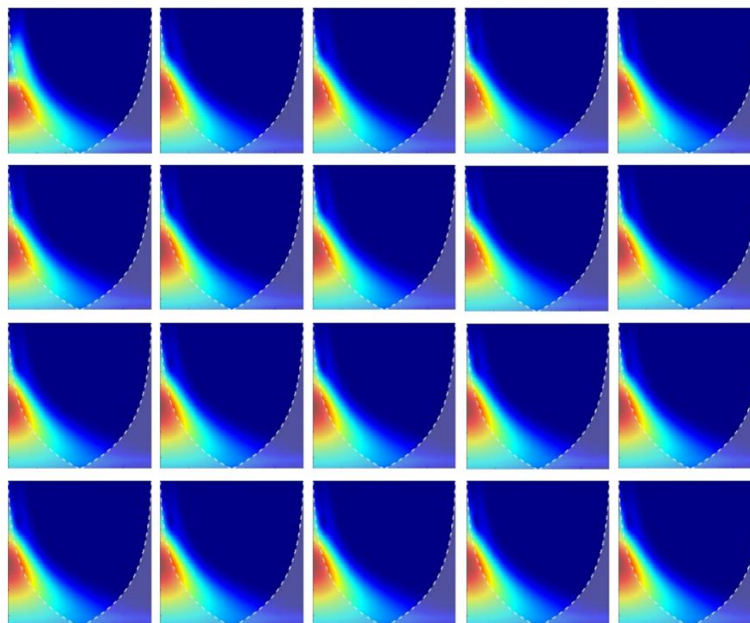


Fig. 13. Voltage wavelet images of the PV system panels for shading fault.

5. DEEP LEARNING MODELS FOR FAULT DETECTION AND LOCALIZATION

The performance of deep learning fault detection and classification is based on mathematical tools and process models [41]. With the development of deep networks, high-level and abstract features can be derived from the data. For fault classification or regression, it is possible to achieve better results when the effective feature representation of the data is relatively extracted. The convolutional neural network (CNN) consists of three layers: the convolutional layer (CL), the pooling layer (PL), and the fully connected layer (FCL) [42].

The convolutional layer extracts features from the input data and upper layer features by combining multiple convolutional kernels, multiplying the input features with matrix elements, and adding the deviation from the input. It is possible to extract local spatial correlation features from the input information by adjusting the size of the convolution kernel in the convolution layer, thus enhancing some features while reducing noise effects [13].

Using a pooling layer, the size of convolution features is reduced. In order to reduce the computational power needed to process the data, dimensionality reduction schemes are used. In addition, it ensures effective training by extracting rotational and positional invariant features [43]. Learning nonlinear combinations of high-level features is most effective with fully connected layers [44]. Fault detection and classification using CNNs has the following advantages:

- CNN inputs can include time series, spectrograms, and images, leading to multi-source heterogeneity of industrial system data [45].
- With CNN features, the diagnosis algorithm is more robust and can generalize better due to translation invariance. In PV systems, this is particularly important since PV systems are often accompanied by strong magnetic interference and high temperatures [46].
- Fault analysis in PV systems is often impossible due to the large amount of data they generate in real time. Small sample sizes can be generated by learning the probability distribution of real data [47].

Deep learning approach classifies a dataset based on the classified features of twenty PV panels in the given simulation design in order to classify them into four different classes: normal, open-circuit, short-circuit, and shading. Two models are used in deep learning.

The first uses the current parameter and the second uses the voltage parameter. Both models are implemented with three different types of deep neural networks in MATLAB, namely GoogleNet, SqueezeNet, and ResNet-50.

GoogleNet is a 22-layer deep CNN. It is used to solve image classification and object detection tasks. The input layer in the GoogLeNet architecture takes an image with dimensions 224×224 [48]. SqueezeNet is an 18-layer deep CNN. It uses design strategies to reduce the number of parameters. It is used to classify images. The input layer in SqueezeNet takes an image with dimensions 227×227 [49]. While ResNet-50 is a 50-layer deep CNN.

It consists of 48 convolutional layers, one MaxPool layer, and one intermediate pooling layer. It is used for image classification problems. The input layer of the network takes an image with dimensions 224×224 [50].

The dataset consists of 1220 images and is divided into two parts; 70% is used for learning, which is equivalent to (854 images), and 30% is used for testing accuracy, which is equivalent to (366 images). All networks use 30 epochs, a batch size of 40, with an initial rate of 0.0001, and a verification frequency of 50. Three different convolutional neural networks are used to train and validate the images of wavelet transform of the panels current.

6. RESULTS

The results showed that the accuracy of GoogleNet and ResNet-50 is 99.73%, which is the best compared to SqueezeNet, which has a shorter learning time. As a result, when using the current wavelet transform, GoogleNet is the best because it has the highest accuracy and moderate training time, as shown in Table 6.

Table 6. Comparison between GoogleNet, SqueezeNet, and Resnet50 with current wavelet transform.

| Model No. | Net | Time to train | Accuracy |
|-----------|-------------|---------------|----------|
| 1 | GoogleNet, | 68 min 34 s | 99.73% |
| 2 | SqueezeNet, | 34 min 56 s | 99.18% |
| 3 | ResNet-50 | 175 min 59 s | 99.73% |

Table 7 shows the comparison between different CNNs when the wavelet transform of the panels voltage. The results show that the accuracy of GoogleNet and SqueezeNet is 99.45%, which is the lowest. ResNet-50 has the highest accuracy but requires a longer learning time. As a result, when using voltage wavelet transform, ResNet-50 is the best because it has the highest accuracy of 100% and suitable training time.

Table 7. Comparison between GoogleNet, SqueezeNet, and Resnet50 with voltage wavelet transform.

| Model No. | Net | Time to Train | Accuracy |
|-----------|------------|---------------|----------|
| 1 | GoogleNet | 21 min 16 s | 99.45% |
| 2 | SqueezeNet | 11 min 45 s | 99.45% |
| 3 | ResNet-50 | 54 min 3 s | 100% |

Fig. 14 shows the accuracy and loss achieved for the current wavelet transform model when using GoogleNet, showing that the accuracy is 99.73%. While Fig. 15 shows the accuracy and loss achieved for the voltage wavelet transform model when using ResNet-50, showing that the accuracy is 100%.

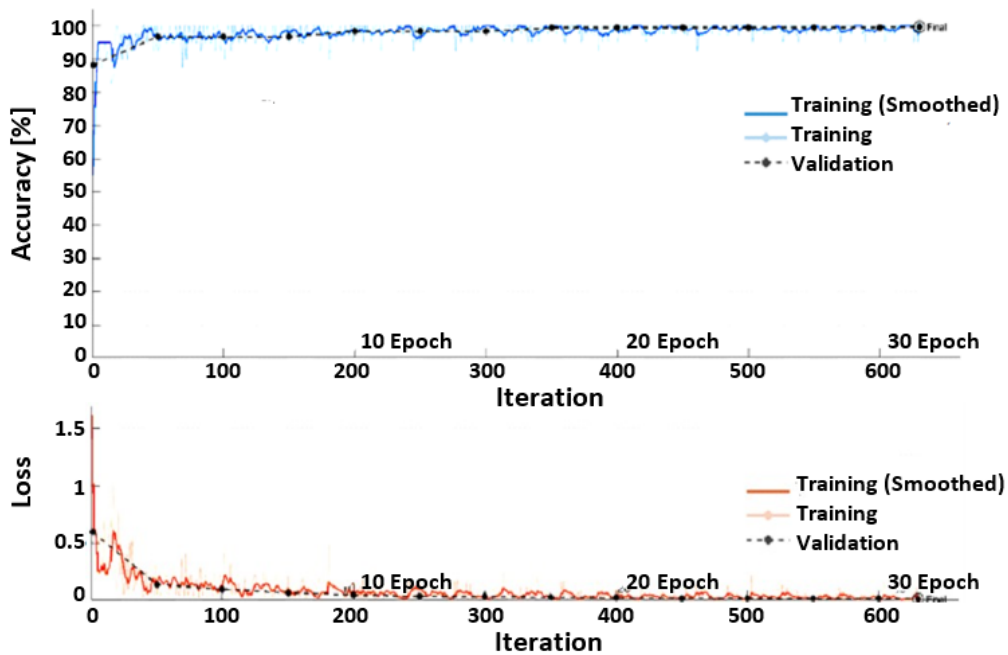


Fig. 14. The accuracy and loss when using current wavelet transform with GoogleNet.

When comparing the model based on current wavelet transform with the model based on voltage wavelet transform, the results show that the voltage based model is more accurate when using ResNet-50 which is 100% and has shorter time to train compared with current based model. The confusion matrix of the pre-trained network of the voltage wavelet transform when using ResNet-50 is shown in Fig. 16. The first four diagonal cells show the number and percentage of correct classifications by the trained network. Obviously, 324 normal cases (30% of 1080 images) were correctly classified as normal. This corresponds to 88.5% of the total 366 images (30% of 1220 images). Likewise, 30 cases were correctly classified as open circuit fault. This corresponds to 8.2% of all images. Also, 6 cases were correctly classified as short circuit fault. This corresponds to 1.6% of all images, and this cell is the same for the shading fault. Out of 324 normal predictions, 100% are correct. Out of the 30 open circuit fault predictions, 100% were correct. Out of the 6 short circuit faults, 100% were predicted correctly. Out of the 6

shading errors, 100% of them were classified correctly. In general, 100% of the predictions are correct by using the proposed deep learning approach.

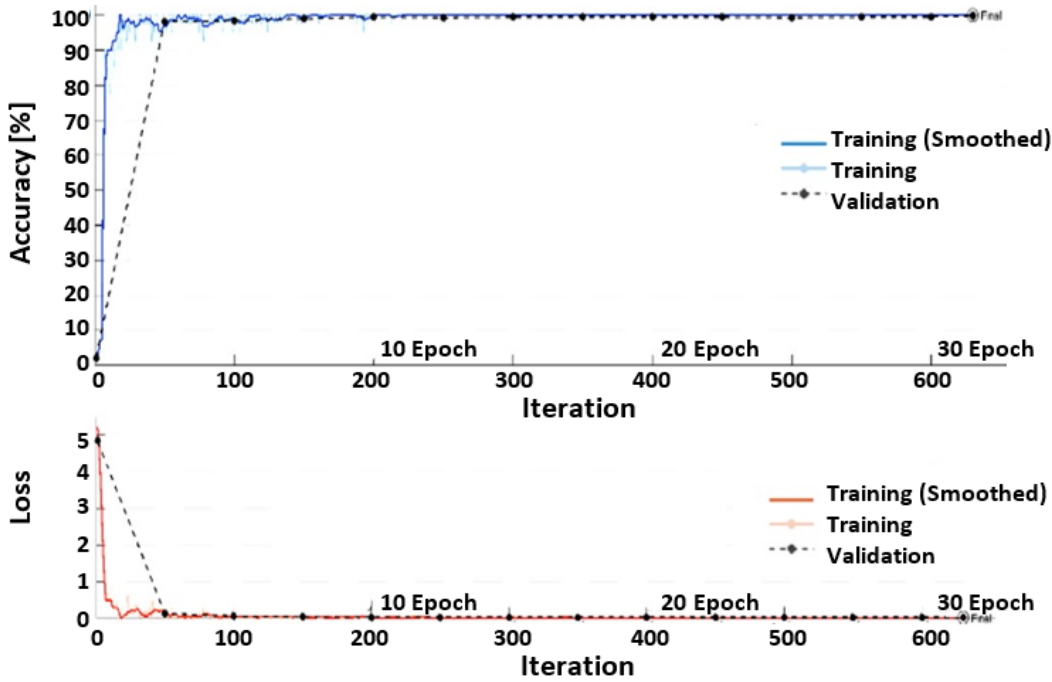


Fig. 15. The accuracy and loss when using voltage wavelet transform with ResNet-50.

| | | | | | | |
|--------------|---------------|--------------|---------------|--------------|--------------|--------------|
| Output Class | Normal | 324 88.5% | 0 0.0% | 0 0.0% | 0 0.0% | 100% 0.0% |
| | Open Circuit | 0 0.0% | 30 8.2% | 0 0.0% | 0 0.0% | 100% 0.0% |
| | Short Circuit | 0 0.0% | 0 0.0% | 6 1.6% | 0 0.0% | 100% 0.0% |
| | Shading | 0 0.0% | 0 0.0% | 0 0.0% | 6 1.6% | 100% 0.0% |
| | | 100% 0.0% | 100% 0.0% | 100% 0.0% | 100% 0.0% | 100% 0.0% |
| | Normal | Open circuit | Short circuit | Shading | | |
| | Target Class | | | | | |

Fig. 16. The confusion matrix of the pre-trained network of voltage wavelet transforms with ResNet-50.

7. CONCLUSIONS

The research utilized deep learning method in detecting, classifying and locating faults in PV systems. It is mainly based on MATLAB simulation of the PV system as well as real-time measurements of current and voltage. The deep learning approach classifies a dataset - based on the classified features of PV panels - into four different categories: normal circuit, open-circuit, short-circuit, and shading. Two deep learning models were proposed; the first one is based on current parameters and the second is based on voltage parameters. Both models are

implemented using three different types of deep neural networks, namely GoogleNet, SqueezeNet, and ResNet-50. The dataset is divided into two parts: 70% is used for learning and 30% is used for testing accuracy. The proposed deep learning methods showed to be effective and accurate in detecting, classifying and locating three types of faults (open-circuit, short-circuit, and shading). The results indicate that the deep learning method based on Resnet50 and voltage images was 100% accurate with a training time of 55 min to classify and identify faults, while the accuracy reached 99.73% with a significant increase in training time (176 min) when using the deep learning approach based on current images. Because the voltage parameter has the best accuracy scenario, this parameter is sent from each panel to the main computer to be converted into an image, and then use the ResNet-50 model. Therefore, each panel can be detected and classified, and by numbering each panel, the location of the defect can be determined.

Troubleshooting a PV system is extremely important, especially when it is on a large scale or in rural areas. This method can be applied in large-scale PV systems with different defects, and different parameters. As future work, current wavelets and voltage wavelets can be combined and used with deep learning to detect, classify and locate faults. The method can be applied to a real PV system using the IoT technology.

REFERENCES

- [1] N. Sapountzoglou, B. Raison, "A grid connected PV system fault diagnosis method," IEEE International Conference on Industrial Technology, 2019, doi: 10.1109/ICIT.2019.8755166.
- [2] M. Obaidi, N. Derbel, "IoT-based monitoring and shading faults detection for a PV water pumping system using deep learning approach," Bulletin of Electrical Engineering & Informatics, vol. 12, no. 5, pp. 2673-2681, 2023, doi: 10.11591/eei.v12i5.4496.
- [3] S. Madeti, "A monitoring system for online fault detection in multiple PV arrays". Renewable Energy Focus, vol. 41, pp. 160-178, 2022, doi: 10.1016/j.ref.2022.03.001.
- [4] E. Meyer, E. Dyk, "Assessing the reliability and degradation of PV module performance parameters". IEEE Transactions on Reliability, vol. 53, no. 1, pp. 83-92, 2004, doi: 10.1109/TR.2004.824831.
- [5] I. Alsudi, "Deep-learning based faults detection and classification in PV systems," MSc Thesis, Mechatronics Engineering Department, Philadelphia University, Jordan, 2023.
- [6] A. Appiah, X. Zhang, B. Ayawli, F. Kyeremeh, "Review and performance evaluation of PV array fault," Hindawi-International Journal of Photoenergy, vol. 2019, p. 19, 2019, doi: 10.1155/2019/6953530.
- [7] L. Chen, S. Li, X. Wang, "Quickest fault detection in PV systems," IEEE Transactions on Smart Grid, vol. 9, no. 3, pp. 1835 - 1847, 2016, doi: 10.1109/TSG.2016.2601082.
- [8] M. Benghanem, A. Mellit, C. Moussaoui, "Embedded hybrid model (CNN-ML) for fault diagnosis of PV modules using thermographic images," Sustainability, vol. 15, no 10, p. 7811, 2023, doi:10.3390/su15107811.
- [9] A. Triki-Lahiani, A. Abdelghani, S. Belkhodja, "Fault detection and monitoring systems for PV installations: a review," Renewable and Sustainable Energy Reviews, vol. 82, no. 3, pp. 2680-2692, 2018, doi: 10.1016/j.rser.2017.09.101.
- [10] K. Al-Aubidy, A. Al-Mutairi, H. Al-Kashashneh, "IoT based remote laboratory for solar energy experiments: design and implementation," 18th International Multi-Conference on Systems, Signals and Devices, 2021, doi: 10.1109/SSD52085.2021.9429384.

- [11] H. Zhou, Q. Liu, K. Yan, Y. Du, "Deep learning enhanced solar energy forecasting with AI-driven IoT," *Wireless Communications and Mobile Computing*, vol. 2021, pp. 1-11, 2021, doi: 10.1155/2021/9249387.
- [12] H. Al-Kashashneh, K. Al-Aubidy, "Wireless sensor network based real-time monitoring and fault detection for PV systems," *16th International Multi-Conference on Systems, Signals and Devices*, 2019, doi: 10.1109/ssd.2019.8893245.
- [13] F. Aziz, A. Haq, S. Ahmad, Y. Mahmoud, M. Jalal, U. Ali, "A novel convolutional neural network-based approach for fault classification in PV arrays," *IEEE Access*, vol. 8, pp. 41889-41904, 2020, doi: 10.1109/access.2020.2977116.
- [14] S. Rao, A. Spanias, C. Tepedelenlioglu, "Solar array fault detection using neural networks," *IEEE International Conference on Industrial Cyber Physical Systems*, 2019, doi: 10.1109/icphys.2019.8780208.
- [15] M. Hajiabadi, M. Farhadi, V. Babaiyan, A. Estebarsari, "Deep learning with loss ensembles for solar power prediction in smart cities," *Smart Cities*, vol. 3, no. 3, pp. 842-852, 2020, doi: 10.3390/smartcities3030043.
- [16] H. Zhou, Q. Liu, K. Yan, Y. Du, "deep learning enhanced solar energy forecasting with AI-driven IoT," *Wireless Communications and Mobile Computing*, vol. 2021, pp. 1-11, 2021, doi: 10.1155/2021/9249387.
- [17] G. Almonacid-Ollerros, G. Almonacid, J. Fernandez-Carrasco, M. Espinilla-Estevez, J. Medina-Quero, "A new architecture based on IoT and machine learning paradigms in PV systems to nowcast output energy," *Sensors*, vol. 20, no. 15, p. 4224, 2020, doi: 10.3390/s20154224.
- [18] G. Almonacid-Ollerros, G. Almonacid, J. Fernandez-Carrasco, J. M. Quero, "Opera.DL: deep learning modelling for PV system monitoring" *Proceedings*, vol. 31, no. 1, p. 50, 2019, doi: 10.3390/proceedings2019031050.
- [19] Y. Y-Hong, R. A.Pula, "Methods of PV fault detection and classification: a review," *Energy Reports*, vol. 8, pp. 5898-5929, 2022, doi: 10.1016/j.egy.2022.04.043.
- [20] S. Madeti, S. Singh, "A comprehensive study on different types of faults and detection techniques for solar PV system," *Solar Energy*, vol. 158, pp. 161-185, 2017, doi: 10.1016/j.solener.2017.08.069.
- [21] M. Cubukcu A. Akanalci, "Real-time inspection and determination methods of faults on PV power systems by thermal imaging in Turkey," *Renewable Energy*, vol. 147, p. 1231-1238, 2020, doi: 10.1016/j.renene.2019.09.075.
- [22] J. Haney A. Burstein, "PV system operations and maintenance fundamentals," 2013, *Solar America Board for Codes and Standards*, <http://www.solarabcs.org/about/publications/reports/operations-maintenance/pdfs/Solar ABCs -35-2013.pdf>.
- [23] M. Akram, G. Li, Y. Jin, X. Chen, "Failures of PV modules and their detection: a review," *Applied Energy*, vol. 313, p. 118822, 2022, doi: 10.1016/j.apenergy.2022.118822.
- [24] T. Kirchartz, A. Helbig, W. Reetz, M. Reuter, J. Werner, U. Rau, "Reciprocity between electroluminescence and quantum efficiency used for the characterization of silicon solar cells," *Progress in PVs Research and Applications*, vol. 17, no. 6, pp. 394-402, 2009, doi: 10.1002/pip.895.
- [25] G. Benatto, C. Mantel, S. Spataru, A. Lancia, N. Riedel, S. Thorsteinsson, P. Poulsen, H. Parikh, S. Forchhammer, D. Sera, "Drone-based daylight electroluminescence imaging of PV modules," *IEEE Journal of PVs*, vol. 10, no. 3, pp. 872-877, 2020, doi: 10.1109/JPHOTOV.2020.2978068.
- [26] T. Takashima, J. Yamaguchi, K. Otani, K. Kato, M. Ishida, "Experimental studies of failure detection methods in PV module strings," *IEEE 4th World Conference on PV Energy Conference*, Waikoloa, 2006, doi: 10.1109/WCPEC.2006.279952.
- [27] J. Solórzano, M. Egido, "Automatic fault diagnosis in PV systems with distributed MPPT," *Energy Conversion and Management*, vol. 76, pp. 925-934, 2013, doi: 10.1016/j.enconman.2013.08.055.

- [28] M. Alajmi, K. Awedat, M. Aldeen, S. Alwagdani, "IR thermal image analysis: an efficient algorithm for accurate hot-spot fault detection and localization in solar PV systems," *IEEE International Conference on Electro Information Technology*, 2019, doi: 10.1109/eit.2019.8833855.
- [29] P. Ducange, M. Fazzolari, B. Lazzarini, F. Marcelloni, "An intelligent system for detecting faults in PV fields," *11th IEEE International Conference on Intelligent Systems Design and Applications*, 2011, doi: : 10.1109/ISDA.2011.6121846.
- [30] W. Chine, A. Mellit, V. Lughi, A. Malek, G. Sulligoi A. Pavan, "A novel fault diagnosis technique for PV systems based on artificial neural networks," *Renewable Energy*, vol. 90, pp. 501-512, 2016, doi: 10.1016/j.renene.2016.01.036.
- [31] F. Aziz, A. Haq, S. Ahmad, Y. Mahmoud, M. Jalal, U. Ali, "A novel convolutional neural network-based approach for fault classification in PV arrays," *IEEE Access*, vol. 8, pp. 41889-41904, 2020, doi: 10.1109/access.2020.2977116.
- [32] L. Bonsignore, M. Davarifar, A. Rabhi, G. Tina, A. Elhajjaji, "Neuro-Fuzzy fault detection method for PV systems," *Energy Procedia*, vol. 62, pp. 431-441, 2014, doi: 10.1016/j.egypro.2014.12.405.
- [33] X. Li, Q. Yang, Z. Lou, W. Yan, "Deep learning based module defect analysis for large-scale PV farms," *IEEE Transactions on Energy Conversion*, vol. 34, no. 1, pp. 520-529, 2019, doi: 10.1109/tec.2018.2873358.
- [34] L. Sandjakoska, F. Stojanovska, "How initialization is related to deep neural networks generalization capability: experimental study," *55th International Scientific Conference on Information, Communication and Energy Systems and Technologies*, 2020, doi: 10.1109/icest49890.2020.9232882.
- [35] S. Venkatesh, V. Sugumaran, "Fault detection in aerial images of PV modules based on deep learning," *IOP Conference Series: Materials Science and Engineering*, 2021, doi: 10.1088/1757-899x/1012/1/012030.
- [36] S. Zaki, H. Zhu, M. Al Fakih, A. Sayed, J. Yao, "Deep-learning-based method for faults classification of PV system," *IET Renewable Power Generation*, vol. 15, no. 1, pp. 193-205, 2021, doi: 10.1049/rpg2.12016.
- [37] B. Du, Y. He, Y. He, J. Duan, Y. Zhang, "Intelligent classification of silicon PV cell defects based on eddy current thermography and convolution neural network," *IEEE Transactions on Industrial Informatics*, vol. 16, no. 10, pp. 6242 - 6251, 2020, doi: 10.1109/TII.2019.2952261.
- [38] X. Li, W. Li, Q. Yang, W. Yan, A. Zomaya, "An unmanned inspection system for multiple defects detection in PV plants," *IEEE Journal of PVs*, vol. 10, no. 2, pp. 568 - 576, 2020, doi: 10.1109/JPHOTOV.2019.2955183.
- [39] Z. Chen, Y. Chen, L. Wu, S. Cheng, P. Lin, "Deep residual network based fault detection and diagnosis of PV arrays using current-voltage curves and ambient conditions," *Energy Conversion and Management*, vol. 198, no. 111793, 2019, doi: 10.1016/j.enconman.2019.111793.
- [40] S. Cheng, P. Chi-man, "3D multi-resolution wavelet convolutional neural networks for hyperspectral image classification," *Information Sciences*, vol. 420, pp. 49-65, 2017, doi: 10.1016/j.ins.2017.08.051.
- [41] M. Mirnaghi, F. Haghghat, "Fault detection and diagnosis of large-scale hvac systems in buildings using data-driven methods: a comprehensive review," *Energy and Buildings*, vol. 229, no. 110492, 2020, doi: 10.1016/j.enbuild.2020.110492.
- [42] J. Ni, T. Young, V. Pandelea, F. Xue, E. Cambria, "Recent advances in deep learning based dialogue systems: a systematic survey," *International Journal of Machine Learning and Cybernetics*, vol. 56, pp. 3055-3155, 2023, doi: 10.1007/s10462-022-10248-8.
- [43] A. Khan, A. Sohail, U. Zahoora, A. Qureshi, "A Survey of the Recent architectures of deep convolutional neural networks," *Artificial Intelligence Review*, vol. 53, p. pages5455-5516, 2020.

- [44] X. Lu, P. Lin, S. Cheng, Y. Lin, Z. Chen, L. Wu, Q. Zheng, "Fault diagnosis for PV array based on convolutional neural network and electrical time series graph," *Energy Conversion and Management*, vol. 196, pp. 950-965, 2019, doi: 10.1016/j.enconman.2019.06.062.
- [45] Y. Ma, L. Zhao, Y. Zhang, Q. Zhou, M. Zhang, S. Yang, "Multi-objective optimal scheduling of power systems based on complementary characteristics of heterogeneous energy sources," *4th Conference on Energy Internet and Energy System Integration*, 2020, doi: 10.1109/EI250167.2020.9347052.
- [46] E. Kauderer-Abrams, "Quantifying translation-invariance in convolutional neural networks," *ArXiv*, vol. 1801.01450, 2018, doi: 10.48550/arXiv.1801.01450.
- [47] S. Razak, B. Jafarpour, "Convolutional neural networks (CNN) for feature-based model calibration under uncertain geologic scenarios," *Computational Geosciences*, vol. 24, p. 1625-1649, 2020, doi: 10.1007/s10596-020-09971-4.
- [48] C. Szegedy, W. Liu, Y. Jia, P. Sermanet, S. Reed, D. Anguelov, D. Erhan, V. Vanhoucke, A. Rabinovich, "Going deeper with convolutions," *arXiv*, vol. 1409.4842, 2014, doi: 10.48550/arXiv.1409.4842.
- [49] F. Iandola, S. Han, M. Moskewicz, K. Ashraf, W. Dally, K. Keutzer, "SqueezeNet: AlexNet-level accuracy with 50x fewer parameters and <0.5MB model size," *arXiv*, vol. 1602.07360, 2016, doi: 10.48550/arXiv.1602.07360.
- [50] K. He, X. Zhang, S. Ren, J. Sun, "Deep residual learning for image recognition," *arXiv*, vol. 1512.03385, pp. 770-778, 2016, doi: 10.48550/arXiv.1512.03385.